ChemPubSoc Europe

DOI: 10.1002/cplu.201500326

CHEMPLUSCHEM Full Papers

Effect of Treatment Methods on Chitin Structure and Its Transformation into Nitrogen-Containing Chemicals

Xi Chen,[a] Yongjun Gao,[a] Lan Wang,[b] Hongzhang Chen,[b] and Ning Yan*[a]

Chitin treatment using different methods, including ball mill grinding, steam explosion, alkaline treatment, phosphoric acid, and ionic liquid (IL) dissolution/reprecipitation have been systematically investigated. The chitin structures were thoroughly investigated by using a series of analytical techniques, and the reactivity after each treatment was evaluated in dehydration and liquefaction reactions. The parallel studies enable direct comparisons of these methods and help to establish the structure–activity correlations. Ball mill grinding in dry mode was the most effective method, with the crystal size and the hydrogen-bond network being the two crucial factors in enhancing the reactivity. Remarkably, the yield of 3-acetamido-5-acetylfuran (3A5AF) from chitin dehydration increased to the highest amount (28.5%) after ball mill grinding (the previous record yield was 7.5% for untreated chitin).

Introduction

With increasing concern over fossil fuel depletion, significant efforts have been paid to biomass resources for the sustainable production of biofuels and biochemicals.[1] To achieve an economically feasible method of biorefinery, it is essential to build diversified, high-value bioproduct chains. Currently, biomass utilization is largely focused on woody biomass materials such as cellulose and lignin.[2] Nevertheless, it is highly desirable and beneficial to explore new types of biomass resources to complement and expand the current biorefinery scheme.[3] Chitin, which is the world's most abundant amino-biopolymer with 7 wt% biologically fixed nitrogen, represents a promising raw material to produce value-added biochemicals, especially nitrogen-containing (N-containing) compounds that are not readily available from lignocellulosic biomass. The industrial production of chitin is conducted by extraction of crab and shrimp shells, which are shellfish waste in the fishing industry. As such, chitin valorization not only has scientific importance and potential economic value, but also environmental benefits.

The structure of chitin is similar to that of cellulose except for the side chain at the C-2 position (see Scheme 1). Chitin is a linear polymer of β(1→4)-linked 2-acetamido-2-deoxy-D-glucopyranose. The side chain at the C-2 position is either an acetyl amide group or an amine group. Chitin is highly crystallized with extensive hydrogen-bond networks among the polymer chains, thus making it even more difficult to be dissolved and converted than cellulose. So far, only a handful of studies have been reported that dealt with chitin conversion into chemicals.[4] The non-N-containing chemicals levulinic acid (LA)[5] and 5-hydroxymethylfurfural (5-HMF)[4b] were obtained in water with metal salt additive or concentrated $ZnCl_2$ solution with 11.5 and 9% yield, respectively. Direct chitin dehydration and liquefaction into N-containing compounds were reported very recently.[6] The N-containing furan derivative, 3-acetamido-5-acetylfuran (3A5AF), was produced by chitin dehydration in organic solvent or IL[6a,c] with a maximum yield of 7.5%. In these studies, the yields of target products were relatively low. In chitin dehydration there was no further increase in 3A5AF by employing high temperatures and prolonged reaction times. It indicates that the traditional technologies in the petroleum refinery that are defined by high-temperature processes are inherently not suitable for biorefinery because of the huge structural differences between fossil fuels and biomass materials. Chitin is a highly rigid and functionalized polymeric material, and severe side reactions will happen under harsh conditions. The direct production of chitin into high-yield N-containing products is still challenging.

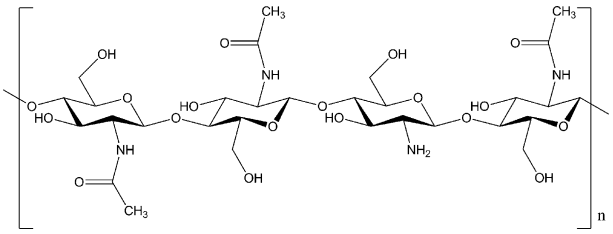

Scheme 1. The chemical structure of chitin polymer.

As far as we are concerned, the greatest challenge in biomass conversion often arises from the high crystallinity and rigidly fixed polymer chains. Logically, a plausible way to enhance

[a] X. Chen, Dr. Y. Gao, Prof. N. Yan
Department of Chemical and Biomolecular Engineering
National University of Singapore
4 Engineering Drive 4, Singapore 117585 (Singapore)
E-mail: ning.yan@nus.edu.sg

[b] Dr. L. Wang, Prof. H. Chen
Institute of Processing Engineering
Chinese Academy of Sciences
1 Zhongguancun North 2nd Alley, Haidian, Beijing 100190 (P. R. China)

Supporting information for this article is available on the WWW under http://dx.doi.org/10.1002/cplu.201500326.

Part of a Special Issue to celebrate Singapore's Golden Jubilee. To view the complete issue, visit: http://dx.doi.org/10.1002/cplu.v80.8.

the reactivity of chitin is to damage the structure robustness and create more flexible polymer chains prior to chemical transformation. The advances in treatment methods[7] (e.g., ball mill, steam explosion, acid/alkaline impregnation, and ionic liquid (IL) treatment) to process biomass materials have been widely reported. These hold promise in applications to enhance chitin-based refinery into N-containing chemicals. In this study, a systematic comparative study of five different methods on the structure change and subsequent chemical reactivity of chitin biomass were conducted, which enables horizontal analysis to identify the most effective method as well as the key factors responsible for chitin conversion. After different treatments, the native chitin and treated samples were comprehensively characterized by various techniques such as scanning electron microscopy (SEM), Brunauer–Emmett–Teller (BET), X-ray powder diffraction (XRD), Fourier transform infrared spectroscopy (FTIR), nuclear magnetic resonance (NMR) spectroscopy, and gel permeation chromatography (GPC). Subsequently, reactivity was studied by investigating two different chemical reactions including chitin dehydration and liquefaction. On the basis of the structure changes and reaction performances, the major structure factors associated with enhanced product yields were summarized, and the relative effectiveness of various treatment methods was compared. The results indicate that different treatment methods endow chitin with substantially different structure changes and reactivity. With the proper method, chitin can be converted with much higher efficiency under milder reaction conditions.

Results and Discussion

Abbreviations were given to the samples treated by different methods. Samples processed by ball mill grinding, steam explosion, alkaline treatment, phosphoric acid, and ionic liquid (IL) dissolution/reprecipitation are denoted as BM, SE, Acid, Base, and IL samples, respectively. Note that there are two modes (dry and wet) for the ball-mill method, thus resulting in two BM samples. BM-1 refers to the sample processed in the dry mode, and BM-2 refers to the sample obtained in the wet mode. As a result, in the following part, the structure changes of the six treated samples are discussed relative to the untreated chitin. The details of treatment procedures are provided in the Experimental Section.

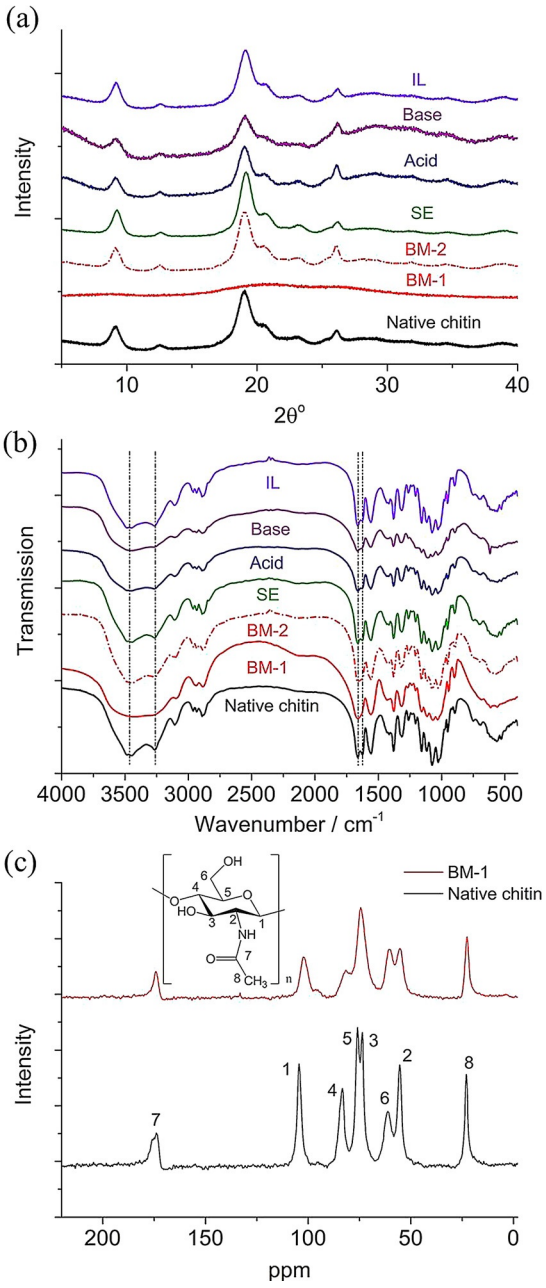

Figure 1. (a) XRD analysis of native and treated chitin samples. (b) FTIR analysis of native and treated chitin samples. (c) Solid-state ^{13}C NMR spectra of the native and BM dry chitin.

Analysis of structure changes using XRD, FTIR, and NMR spectroscopy

XRD and FTIR analyses were conducted on the native chitin and treated samples (as shown in Figure 1), and the calculated crystalline index (CI) parameters are shown in Table 1 (an overall summary). The results of ball-mill-treated chitin and other samples were compiled for comparison. In the XRD pattern of native chitin, the major peak at $2\theta = 19^{\circ}$ represents the (110) plane of crystalline chitin. Native chitin is highly crystalline with a CI value of 91%. In Figure 1a, it is clear that the BM-1 sample displayed significantly decreased crystallinity, and the CI value was reduced strikingly from 91 to 28%. However, only a slight decrease (about a 10% drop) in the CI value was observed for Acid and Base samples, whereas a negligible change was noticed for other samples. Note that BM-2 is much less affected than BM-1, which suggests that the treatment is very sensitive to ball-mill modes. It is plausible that the presence of water mitigates the contact attrition and thus decreases the grinding efficiency. The decrease in the CI values of the Acid, Base, and BM-1 samples was reported in previous studies with cellulose/chitin,[8] whereas the result in our study suggested ball milling to be significantly more efficient than other methods. The IL sample displayed a negligible change in crystal structure, which was different from cellulose treatment by

Table 1. Overall summary of the structure of native and treated chitin.

Chitin	XRD CI [%]	GPC MW [kDa]	BET Surface area [$m^2 g^{-1}$]	FTIR Hydrogen-bond networks	SEM Particle size
native	91	–	7.4	–	–
BM-1	28	↓↓	2.3	decrease	decrease
BM-2	89	↓	6.8	unchanged	unchanged
SE	93	↓	6.2	unchanged	unchanged
Acid	82	↓↓	5.2	decrease	decrease
Base	83	→	1.9	decrease	increase
IL	91	→	6.2	unchanged	unchanged

means of IL dissolution/reprecipitation. Significantly decreased crystallinity was often observed[9] in the cellulose structure. For chitin dissolution in ILs, contrary results in XRD analysis were reported. Chitin regenerated from [BMim]Ac (BMim = 1-butyl-3-methylimidazolium chloride) was reported to show greatly decreased XRD signals, thus indicating the damage of crystalline regions after regeneration.[10] In contrast, chitin regenerated from [BMim]Cl and [AMim]Br exhibited strong XRD signals that were comparable to that of the original chitin.[11] Our results were in agreement with the latter reports. It was assumed that regeneration of the crystalline region readily occurs upon precipitation and drying. As such, it appears that the mechanism behind cellulose and chitin treated by IL is different, despite their similar chemical structure.

The FTIR spectra are shown in Figure 1b. Overall, the chemical backbones of the samples were maintained after all treatments. The detailed assignments of peaks for chitin have been illustrated previously.[12] The bands that range from 3200 to 3500 cm^{-1} are ascribed to the inter- and intrahydrogen bonds between the hydroxyl groups. Meanwhile, the peaks located at 1600–1700 cm^{-1} are assigned to the amide I band (two types of hydrogen bonds in a C=O group with the NH group of the adjacent chain and the OH group of the interchain). The bands assigned to these types of hydrogen bonding became apparently broader and smoother for the BM-1 sample, which suggests that the hydrogen-bond networks among chitin polymer molecules have been remarkably impaired.[13] Such changes have also been found in the Acid and Base samples but to a lesser extent. Negligible changes were observed for the rest of the samples. The FTIR results are in perfect agreement with the XRD data. Ball milling is by far the most effective method to destroy the crystalline regions and the networks of the polymer chains in chitin. As the BM-1 sample showed the most prominent decrease in XRD signals, it has been further compared to native chitin by means of solid-state ^{13}C NMR spectroscopic techniques (Figure 1c). Peak broadening was observed in the BM-1 chitin sample, thus indicating a significant decrease in crystallinity, which is in agreement with the XRD and FTIR results. Furthermore, the peak for C-1 shifted from $\delta = 104$ to 102 ppm in the ball-mill-treated chitin, whereas there is no appreciable chemical shift for other peaks. The C-1 position for *N*-acetyl-D-glucosamine (NAG, chitin monomer) and chitin was at $\delta = 95$ and 104 ppm, respectively, in the literature.[14] The chemical shift of C-1 possibly indicated that partial cleavage of chains occurred and more reducing ends have been exposed.

Optimization of ball-milling parameters

The BM-1 sample exhibited the most dramatic decrease in XRD signals. To further understand the ball-milling process, the number of balls, the feedstock mass, the ball-milling time, and speed were varied. The CI value decreased clearly as numbers of balls increased from 10 to 160 (see Figure S1 in the Supporting Information). Furthermore, the increase in substrate loading reduced the milling efficiency, thus leading to less decrease in crystallinity (see Figure S2 in the Supporting Information). With an increase in time from one half to two hours, the CI value decreased accordingly, whereas insignificant changes were found when the ball-milling time was increased further (see Figure S3 in the Supporting Information). To ensure an efficient breakdown of the crystalline region, a relatively high milling speed is needed. At 300 rpm, the CI value showed a negligible decrease. Nevertheless, the decrease became considerable when the speed increased to 600 and 650 rpm (see Figure S4 in the Supporting Information). These results indicated that ball-milling parameters have remarkable influences on chitin treatment and that operational parameters should be carefully selected in future applications. We also followed the temperature change after ball milling. In the presence of 80 balls at 650 rpm, the temperature was 40.6, 50.5, and 50.8 °C, respectively after one half, one, and three hours of milling. In the presence of 160 balls at 650 rpm, the temperature increased to 53 °C after half an hour. The moderate temperature increase during ball milling might play a role in breaking down the interchain hydrogen-bond network in chitin.

Analysis of structure changes using GPC, SEM, and BET

The molecular weights (MWs) were analyzed by using GPC (see Figure S5 in the Supporting Information) and calculated (see Table S1 in the Supporting Information). Both the native and processed samples showed wide MW distributions (high polydispersity). Since all the samples were dissolved and detected under identical conditions, the changes in MW after treatment could be observed and compared. The Base and IL samples had MWs comparable to that of native chitin; SE and BM-2 samples exhibited moderately decreased MW, whereas BM-1 and Acid samples displayed considerably decreased MW. The Base and IL treatments led to samples with the least reduced MW owing to the mild process conditions. The decrease in MW is not unexpected for SE and Acid samples and is consistent with previous studies on cellulose.[15] Steam explosion was conducted with water under elevated temperature and pressure, which caused a moderate decrease. The large decrease in that of the Acid sample was plausible owing to the fact that chitin polymers could be chemically attacked by acid molecules during the process. Ball milling also seems to be effective

in cleavage of chitin polymer chain, plausibly owing to the "hot-point" effect induced by frictions and impacts.[16]

SEM images were first taken at a low magnification of 25× (see Figure S6 in the Supporting Information). It was observed that the particle size of the BM-1 and Acid samples decreased remarkably, a phenomenon that was not observed in other samples.

At high magnification, the treated samples displayed a distinctive morphology: Magnification images of the samples at 3000 and 50000× are shown in Figure S7 in the Supporting Information and Figure 2. At 3000×, SE and IL samples showed an uneven surface similar to native chitin as bulky flakes. Nevertheless, the BM-1, Acid, and Base samples appeared as much smaller flakes. In addition, it seems that pores were generated on the surface of flakes of BM-2 chitin. With the higher magnification of 50000, the fibers and adherent granules could be observed. BM-1 and BM-2 chitin samples showed the existence of chitin fibers but fewer granules. However, IL chitin exhibited distinguished swollen and wider chitin fibers, which was caused by the dissolution process. The SE sample showed highly arranged thinner fibers and granules. For Acid and Base samples, only crowded granules were observed without long-chain fibers. The results showed that the processes modified the chitin particle size and the chitin fiber morphology. BET analysis was conducted to confirm whether pore structure was generated after treatment. The nitrogen sorption isotherms of the samples are shown in Figure S8 in the Supporting Information. The BET surface areas and pore volumes were small for all samples. Unexpectedly, these values of the treated samples showed a general decrease relative to the native chitin. Therefore, the treatment did not induce the generation of a porous structure in chitin.

The overall structure changes of different samples are summarized in Table 1. The BM-1 sample exhibited the most prominent decrease in crystallinity. At the same time, the hydrogen-bond networks and the MW of the BM-1 sample were remarkably reduced as well, whereas the BM-2 sample was less affected. Acid and Base samples showed decreased crystallinity, hydrogen-bond networks, and molecular weights. The particle size of the Acid sample was also reduced. Relative to these samples, less change in the structure was observed for the SE and IL samples.

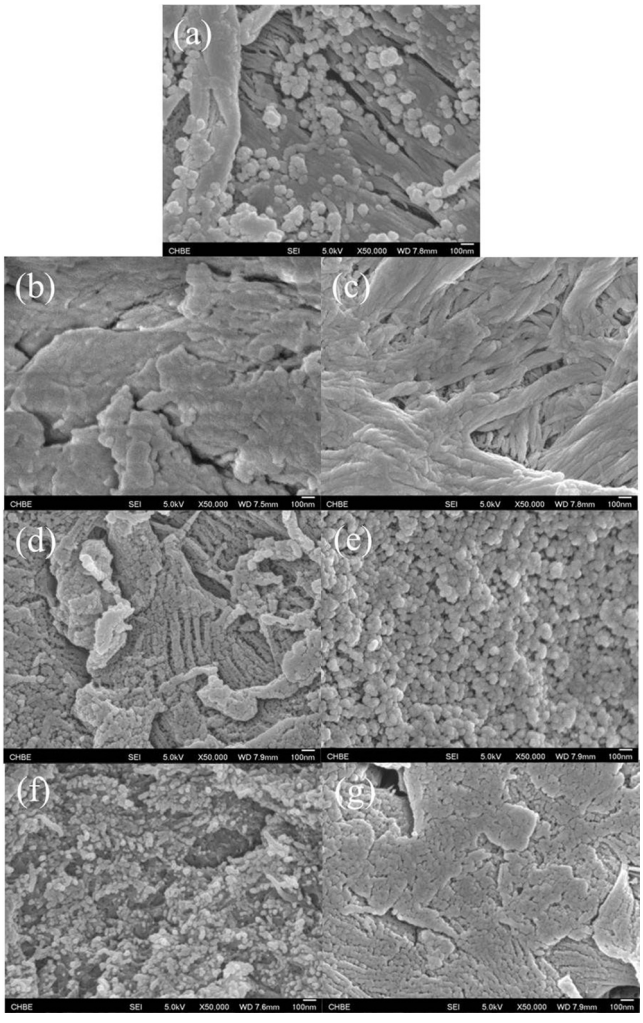

Figure 2. SEM images (×50000) of (a) native chitin; (b) BM-1; (c) BM-2; (d) SE; (e) Acid; (f) Base; and (g) IL.

Transformation performance: Dehydration of native chitin and treated samples

A dehydration reaction was conducted that employed all samples as substrates. Both N-methyl-2-pyrrolidone (NMP) and [BMim]Cl were used as the solvent for chitin depolymerization-dehydration into 3A5AF (shown in Figure 3a). Overall, the IL solvent was superior to the NMP solvent for the transformation. In NMP, the 3A5AF yield of native chitin was 4.6% under the employed conditions. The BM-1 and Acid samples afforded a higher yield of 3A5AF (10.6 and 5.3%, respectively). The SE sample showed a comparable yield (4.8%), whereas the rest showed decreased yields. However, all treated samples exhibited enhanced or at least comparable product yields in [BMim]Cl solvent. Acid and Base samples provided a more than twofold increase in 3A5AF yield; BM-1 chitin achieved the highest yield of 20.2%. Thus, the BM-1 sample was further studied under different conditions (Figure 3b). Rapid initial reaction rates were observed and peak values were reached within just ten minutes. Increasing the temperature to 180 °C while maintaining the reaction time at ten minutes provided the highest 3A5AF yield. Even higher temperatures were not investigated because the decomposition of [BMim]Cl solvent could occur. By means of dry ball milling, the yield of the target product in chitin dehydration was remarkably improved from the previous record of 7.5 to 28.5% (the highest value obtained), with a decreased reaction time from 60 to 10 minutes. Column chromatography was used to separate the product from IL solvent with an isolated yield of around 20%. For scalable production, other feasible separation methods should be considered. It has been reported that 3A5AF can be extracted from IL by using ethyl acetate.[4c] This could be a first separation step.

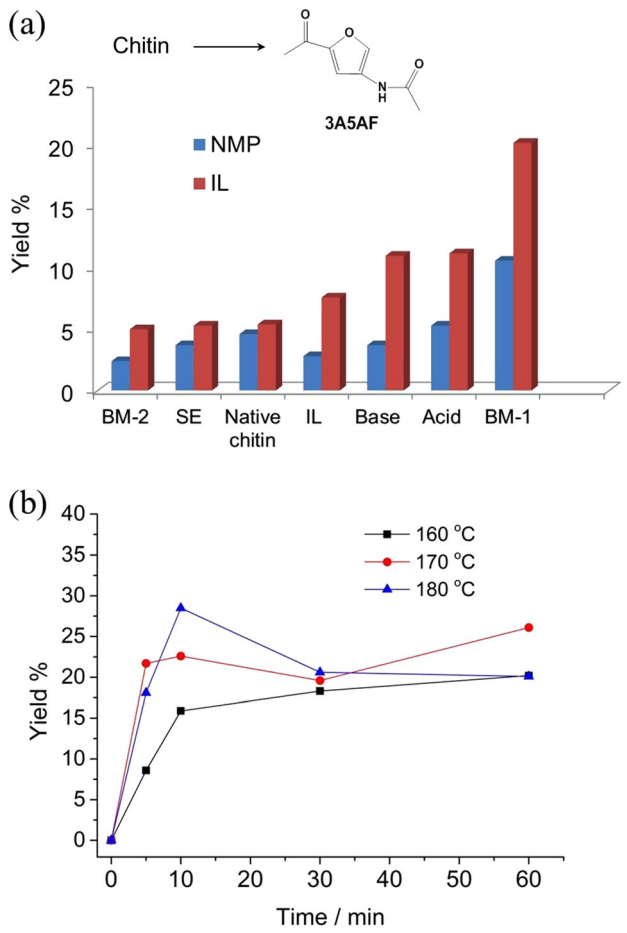

Figure 3. (a) Dehydration of chitin and treated samples. Blue columns in NMP solvent: 215 °C, NMP (3 mL), substrate (100 mg), boric acid (400 mol%), LiCl (200 mol%), HCl (100 mol%), 1 h; red columns in IL solvent: 180 °C, [BMim]Cl (1 g), substrate (80 mg), boric acid (400 mol%), HCl (100 mol%), 1 h. (b) Studies of BM-1 sample in IL solvent under different conditions: [BMim]Cl (1 g), substrate (80 mg), boric acid (400 mol%), HCl (100 mol%), reaction for 5, 10, 30, and 60 min at 160, 170, and 180 °C, respectively.

Table 2. Liquefaction results of chitin and treated samples.

Entry[a]	HADP [%]	HAADP [%]	Conversion [%]
native chitin	6.6	0.9	28.0
BM-1	28.0	4.3	88.7
BM-2	7.9	0.9	13.5
SE	6.7	0.7	27.9
Acid	10.2	3.2	48.2
Base	18.5	4.2	67.2
IL	7.8	2.6	43.5

[a] Reaction conditions: EG (1 g), sulfuric acid (0.08 g; 8% w/w EG), and substrate (0.15 g; 15% w/w EG) at 150 °C for 20 min.

Transformation performance: Liquefaction of native chitin and treated samples

The native and treated chitin samples were also tested in the liquefaction reaction in ethylene glycol (EG) over sulfuric acid at 150 °C. The results were mostly congruous with those in the dehydration reaction (see Table 2). The BM-1, Base, and Acid

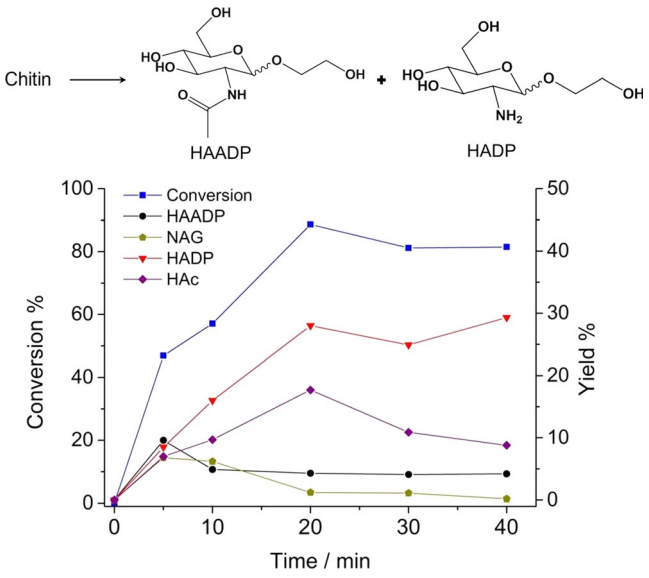

Figure 4. The kinetic profile of liquefaction of BM-1 chitin. Reaction conditions: 1 g EG, 0.08 g sulfuric acid (8% w/w EG), and 0.15 g substrate (15% w/w EG) at 150 °C for 0, 5, 10, 20, 30, and 40 min.

samples afforded more target products of hydroxyethyl-2-amino-2-deoxyhexopyranoside (HADP) and hydroxyethyl-2-acetamido-2-deoxyhexopyranoside (HAADP) than the rest of the samples. The BM-1 sample still afforded the highest total yield of HADP and HAADP (32.3%) with 88.7% liquefaction yield, under much milder conditions than previously reported.[6b] The yields of formed target products follow this order: BM-1 > Base > Acid > IL > BM-2 > native chitin ≈ SE.

Since the BM-1 sample had the best performance, the kinetic profile was investigated further (see Figure 4). The liquefaction reaction quickly reached about 50% chitin conversion within five minutes, and then gradually increased to 88% at 20 minutes. A slight decrease (about 6%) in liquefaction efficiency was observed at 30 and 40 minutes, which might indicate the formation of insoluble char. The chitin monomer was detected during the liquefaction, thus suggesting that the hydrolysis was the first step along the reaction pathway. The yield was about 7% at five minutes and then declined constantly to a yield of 0.2% at 40 minutes. Similarly, the liquefied product HAADP peaked at five minutes (9.6% yield) and then decreased to 4% yield. The major product HADP had a steady increase in the initial 20 minutes and reached a plateau afterwards. A similar trend was also observed for acetic acid (HAc), the yield of which decreased after 20 minutes. Relative to native chitin, the BM-1 sample showed a faster reaction rate, and the peak values were achieved within 20 minutes instead of 60 minutes under lower temperature.

In both dehydration and liquefaction reactions, the BM-1 sample showed the best performance. The Acid and Base samples also exhibited an appreciable increase in product yields. These results, together with the structure characterizations, provide the opportunity to identify the major factors responsible for enhanced reactivity. Considering the apparent decrease in crystal size and hydrogen-bond networks of BM-1, Acid, and

Base samples, these two properties are highly likely to be the essential factors in improving reaction activity. Surface area, however, was not a crucial factor. Molecular weight and particle size might be related to the reaction performance, but this is not conclusive. Interestingly, IL chitin exhibited moderately increased product yields in some cases, despite the only structure change of IL chitin being the morphology change. The SEM image suggested that the chitin fibers swelled after IL treatment, thus indicating that the swelling of chitin polymer is beneficial, to some extent, for the chemical transformation.

Conclusion

This study describes a systematic comparison study of the influences of five treatment methods on chitin structure and chemical reactivity. Different methods exhibited varied effects in changing the structural parameters. We observed a strong correlation between the crystal size/hydrogen-bonding network intensity and the reactivity of chitin. A treatment method that is effective in decreasing the crystal size and hydrogen-bonding network will consequently lead to a considerable increase of chitin reactivity in the subsequent transformations. The dehydration yield was increased from the previous 7.5 to 28.5%. A feasible separation method is needed to separate the product from IL solvent, for example, first by extraction and then further purification. Our study demonstrated that chitin is indeed a promising material for the direct production of N-containing chemicals with high yields after damaging its crystallinity by a proper treatment method.

Experimental Section

Materials and chemicals

Chitin was purchased from Wako Pure Chemical Industry. Boric acid (ACS grade) was purchased from Amresco. Sodium chloride (NaCl, AR grade) was purchased from Schedelco. Lithium chloride (LiCl, 98%) and dimethylacetamide (DMAc, anhydrous, 99.8%) were purchased from Alfa Aesar. Phosphoric acid (H_3PO_4, 85%) and ethylene glycol (EG, >99%) were purchased from VWR Singapore. Sodium hydroxide (NaOH, 99%), acetic acid (HAc, 99%), and hydrochloric acid (HCl, 37%) were purchased from Merck. Urea (ACS grade), hexamethyldisilazane (HMDS, 99%), trifluoreacetic acid (99%), pyridine (AR), *N*-acetyl-D-glucosamine (NAG, 99%), and *N*-methyl-2-pyrrolidone (NMP, anhydrous, 99.5%) were purchased from Sigma–Aldrich. Sulfuric acid (H_2SO_4, 97%) was purchased from J.T. Baker. 1-Butyl-3-methylimidazolium chloride ([BMim]Cl, 99%) and 1-allyl-3-methylimidazolium bromide ([AMim]Br, 99%) were purchased from the Lanzhou Institute of Chemical Physics. All chemicals were used as received.

Protocol for ball milling and steam explosion treatment

Ball-milling samples were obtained under different grinding conditions, including dry and wet modes (denoted as BM-1 and BM-2, respectively). BM-1 chitin was ground in dry mode with a planetary ball mill (PM 100 CM; Retsch) with a chamber volume of 125 mL at 650 rpm and 4 h total mill time (20 min mill and 10 min rest as a cycle). The material of the chamber and balls was zirconium oxide (ZrO_2). The feed quantity was 1 g, and 45 balls with diameter 10 mm were used. BM-2 was ground with a PL11 PFI Beater (PFI Mill) at a speed of 6000 rpm in the presence of 10% water (wet mode). Further optimization of dry ball-milling parameters was conducted with a Pulverisette P7 Premium Line (Fritsch) with a chamber (ZrO_2) volume of 45 mL with 10 min milling and 5 min rest as a cycle. The balls (ZrO_2) had a diameter of 5 mm. The temperature after the ball-milling process was recorded for selected optimization experiments. A thermometer was inserted into the solids and detected the temperature after milling.

Steam explosion was carried out in a 5 L batch reactor (Weihai Automatic Control Reactor Ltd., China). About 200 g of the dried sample were fed into the reactor. Steam was charged into the reactor at 1.5 MPa at 200 °C for 3 min and then released. The resulting chitin contained 50–70% water content because the steam condensed. After the process, the material was dried in a forced-air oven at 60 °C for 24 hours (denoted as the SE sample).

Protocol for acid, base, and IL treatment

H_3PO_4 dissolution/reprecipitation was conducted in the following manner. Chitin (35 mg) was added into an H_3PO_4 solution (1 g, 68 wt%) in a thick-walled glass tube and heated at 60 °C for 1 h with a stirring speed of 700 rpm. Then 10 wt% NaOH was used to neutralize the solution, during which chitin precipitated. The white solid was washed three times with deionized water and dried in oven at 70 °C overnight (denoted as the Acid sample).

The dissolution of chitin in base solution was reported in a previous study,[17] and this process was used for alkaline treatment of chitin. Briefly, chitin (600 mg) was dispersed in an aqueous solution (total 30 g) of NaOH (8 wt%) and urea (4 wt%) in a plastic centrifuge tube. The suspension was kept at −20 °C and stirred twice over 48 h. The solution was centrifuged, and the liquid supernatant was collected. Then the supernatant was neutralized using H_2SO_4 (10 wt%) aqueous solution. Regenerated chitin was precipitated, washed with deionized water until the pH reached 7, and then dried in an oven at 70 °C overnight (denoted as the Base sample).

IL dissolution/reprecipitation was conducted in a similar manner. Chitin (35 mg) was dissolved in [AMim]Br (1.5 g) at 110 °C for 1 h in a thick-walled glass tube with a stirring speed of 600 rpm. Afterwards it was cooled to room temperature, and deionized water (20 mL) was added to precipitate the chitin. The solid was collected by centrifugation, washed three times with deionized water, and then dried in an oven at 70 °C overnight (denoted as the IL sample).

XRD and solid-state ^{13}C NMR spectroscopic analysis

XRD analysis was performed with a Bruker D8 Advance diffractometer with $Cu_{K\alpha}$ radiation at 40 kV. The scan range was from 5 to 40° without rotation. The equation for the CI calculation is shown below [Eq. (1)].[18]

$$CI\ [\%] = (I_{110} - I_{am})/I_{110} \times 100\,\% \quad (1)$$

in which I_{110} is the maximum intensity of the diffraction for the (110) plane at approximately $2\theta = 19.2°$ and I_{am} is the intensity of the amorphous diffraction at approximately $2\theta = 12.7°$.

Native chitin and BM dry chitin samples were sent for solid-state ^{13}C NMR spectroscopic analysis for further comparison. Solid-state

^{13}C NMR spectroscopy was conducted with a Bruker Advance 400 (DRX400) with cross-polarization/magic-angle spinning (CP/MAS).

FTIR and GPC analysis

FTIR was conducted with a Bio-Rad FTS-3500 ARX instrument. Transmission mode was used and the results were collected under N_2 flow. GPC analysis was carried out with a system equipped with a Waters 2410 refractive index detector, a Waters 515 high-performance liquid chromatography (HPLC) pump, and two Waters styragel columns (HT3 and HT4) using 5 wt% LiCl/DMAc as eluent at a flow rate of 0.5 mL min^{-1} at room temperature. The samples were dissolved in the mobile phase solution at 80 °C with rigorous stirring for 2 days under nitrogen atmosphere prior to analysis. The raw data were processed using narrow polydispersity polystyrene standards and calibration using the software Breeze (the calibration curve is shown in Figure S6 of the Supporting Information). Note that the treated samples must be washed thoroughly to remove any acid residues before dissolution. Otherwise, the acid residue would cause decomposition during dissolution and result in much reduced MW values.

SEM and BET analysis

SEM images were obtained with a JEM-6700F scanning electron microscope (JEOL). The sample was immobilized on a copper substrate by conductive adhesives and was coated by platinum before analysis by means of high vacuum evaporation. Gas sorption isotherms were measured using a Micrometrics ASAP 2020 surface area and pore-size analyzer. Prior to the measurement, the samples were outgassed at 100 °C for at least 6 h. The BET specific surface areas were calculated using the adsorption data in the relative pressure (P/P_0) range of 0.05–0.25. The total pore volumes were estimated from the amount adsorbed at a relative pressure P/P_0 of 0.98.

HPLC analysis

HPLC analysis of dehydration product was performed with an Agilent 1200 Series (Agilent Technologies, Germany) LC system by using an Agilent ZORBAX Eclipse carbon-18 column. The mobile phase was 83% water and 17% acetonitrile. The flow rate was kept at 0.5 mL min^{-1} with a run time of 20 min. A UV/Vis detector setting at 230 nm was used to analyze the product. Other products such as HAc and NAG were quantified by HPLC by plotting external calibration curves with standard chemical solutions. HAc was analyzed with an Agilent Hi-Plex H column with 100% H_2SO_4 solution (0.005 M) as the mobile phase, and NAG was analyzed with an Agilent Hi-Plex Ca column with 100% water as the mobile phase. The flow rates were at 0.6 mL min^{-1}, and the UV/Vis detector was set at 210 nm for HAc and 195 nm for NAG.

Gas chromatography (GC) analysis

The major liquefied products were silylated and quantified by using dodecane as the internal standard. The GC analysis was performed with an Agilent 7890 A gas chromatograph with a flame ionization detector (FID) equipped with HP-5 capillary column (30 m × 250 μm). The yield was calculated by using the effective carbon numbers.[19] A general procedure for silylation was as follows.[20] In an analytical vial (1 mL), the product mixture to be analyzed (40 mg), pyridine (700 μL), hexamethyldisilazane (700 μL), trifluoreacetic acid (TFA, 60 μL), and a small stirring bar were added. The closed vial was put in a water bath at 60 °C for 1 h. After silylation, a portion of the reaction mixture (250 μL) and diethyl ether (750 μL) were mixed together and analyzed.

Dehydration of chitin into 3A5AF

Two different solvent systems were attempted for the reaction, including NMP as solvent and IL as solvent. The procedures for chitin dehydration in IL solvent were carried out:[6c] Substrate (80 mg, 0.4 mmol based on the NAG monomer) was placed in a thick-walled glass tube (35 mL). Following that, a magnetic stir bar, boric acid (98 mg, 1.6 mmol), HCl (0.4 mmol), and [BMim]Cl (1 g) were added. In the IL solvent system, HCl instead of NaCl was used together with boric acid as additive because it gave the best results in additive screening. The tube was sealed by a Teflon stopper (with an O ring) and placed into a preheated oil bath at a desired temperature for a certain time at a stirring speed of 700 rpm. The experiments in NMP solvent were conducted in a similar way but with different additives. For product identification and quantification, procedures are provided elsewhere.[6a] The yield of 3A5AF was calculated as follows: product [mol]/starting chitin [mol] × 100%. Since the yield was enhanced significantly in IL solvent after ball-milling treatment, column chromatography was conducted for the isolated yield of the 3A5AF product. Silica gel with particle sizes that ranged from 40 to 63 μm was used as the stationary phase, and 5% methanol and 95% dichloromethane were used as the mobile phase; ball-milled chitin (153 mg) was used as the substrate in IL (1.5 g). After reaction, the solution was reheated to 80 °C to melt the IL and transfer it to the column, whereas the solution was still too viscous to be fully transferred and some of it adhered to the tube wall. After column separation, a yellow-brown solid (25 mg) was obtained, and the solid (≈3 mg) was dissolved in [D_6]DMSO for NMR spectroscopic analysis (see Figure S10 in the Supporting Information). The isolated yield was about 20%.

Liquefaction of chitin into monosaccharides

In a general procedure for chitin liquefaction, chitin or the treated sample (0.15 g, 0.75 mmol) was added with EG solvent (1 g) and 8 wt% H_2SO_4 acid catalyst (80 mg). The mixtures were stirred at 420 rpm and heated for the desired time at 150 °C. After the reaction, the mixtures were cooled and neutralized to pH 7 by using 10 wt% NaOH. Next, the reaction mixture was separated into three (denoted as A, B, and C) fractions, and the major products were separated by HPLC and confirmed by NMR spectroscopy.[6b] Fraction A contained unreacted chitin and was used to determine the conversion. Fractions B and C contained products and were silylated for GC analysis. The yield obtained is based on mole percentage: product [mol]/starting chitin [mol] × 100%.

Acknowledgements

*We thank Prof. Xindong Mu (Qingdao Institute of Bioenergy and Bioprocess Technology, Chinese Academy of Sciences) for supporting this study. This study was financially supported by A*Star, PSF funding with WBS: R-279-000-403-305.*

Keywords: biomass · chitin · homogeneous catalysis · structure–activity relationships · sustainable chemistry

[1] a) D. R. Dodds, R. A. Gross, *Science* **2007**, *318*, 1250 – 1251; b) H. Kobayashi, A. Fukuoka, *Green Chem.* **2013**, *15*, 1740 – 1763; c) E. L. S. Ngee, Y. Gao, X. Chen, T. M. Lee, Z. Hu, D. Zhao, N. Yan, *Ind. Eng. Chem. Res.* **2014**, *53*, 14225 – 14233; d) H. Ben, A. J. Ragauskas, *ACS Sustainable Chem. Eng.* **2013**, *1*, 316 – 324; e) F. Jin, H. Enomoto, *Energy Environ. Sci.* **2011**, *4*, 382 – 397; f) S. Dutta, S. De, B. Saha, *ChemPlusChem* **2012**, *77*, 259 – 272.

[2] a) J. Zhang, J. Teo, X. Chen, H. Asakura, T. Tanaka, K. Teramura, N. Yan, *ACS Catal.* **2014**, *4*, 1574 – 1583; b) S. Siankevich, G. Savoglidis, Z. Fei, G. Laurenczy, D. T. L. Alexander, N. Yan, P. J. Dyson, *J. Catal.* **2014**, *315*, 67 – 74; c) J. Zhang, H. Asakura, J. v. Rijn, J. Yang, P. Duchesne, B. Zhang, X. Chen, P. Zhang, M. Saeys, N. Yan, *Green Chem.* **2014**, *16*, 2432 – 2437; d) S. Siankevich, Z. Fei, R. Scopelliti, G. Laurenczy, S. Katsyuba, N. Yan, P. J. Dyson, *ChemSusChem* **2014**, *7*, 1647 – 1654; e) Y. Gao, J. Zhang, X. Chen, D. Ma, N. Yan, *ChemPlusChem* **2014**, *79*, 825 – 834.

[3] a) X. Chen, N. Yan, *Catal. Surv. Asia* **2014**, 1 – 13; b) F. M. Kerton, Y. Liu, K. W. Omari, K. Hawboldt, *Green Chem.* **2013**, *15*, 860 – 871.

[4] a) M. Mascal, E. B. Nikitin, *ChemSusChem* **2009**, *2*, 859 – 861; b) Y. Wang, C. M. Pedersen, T. Deng, Y. Qiao, X. Hou, *Bioresour. Technol.* **2013**, *143*, 384 – 390; c) M. W. Drover, K. W. Omari, J. N. Murphy, F. M. Kerton, *RSC Adv.* **2012**, *2*, 4642 – 4644; d) M. Osada, K. Kikuta, K. Yoshida, K. Totani, M. Ogata, T. Usui, *Green Chem.* **2013**, *15*, 2960 – 2966; e) F. D. Bobbink, J. Zhang, Y. Pierson, X. Chen, N. Yan, *Green Chem.* **2015**, *17*, 1024 – 1031; f) K. W. Omari, L. Dodot, F. M. Kerton, *ChemSusChem* **2012**, *5*, 1767 – 1772.

[5] K. W. Omari, J. E. Besaw, F. M. Kerton, *Green Chem.* **2012**, *14*, 1480 – 1487.

[6] a) X. Chen, S. L. Chew, F. M. Kerton, N. Yan, *Green Chem.* **2014**, *16*, 2204 – 2212; b) Y. Pierson, X. Chen, F. D. Bobbink, J. Zhang, N. Yan, *ACS Sustainable Chem. Eng.* **2014**, *2*, 2081 – 2089; c) X. Chen, Y. Liu, F. M. Kerton, N. Yan, *RSC Adv.* **2015**, *5*, 20073 – 20080.

[7] a) S. Gandolfi, G. Ottolina, R. Consonni, S. Riva, I. Patel, *ChemSusChem* **2014**, *7*, 1991 – 1999; b) C. K. Nitsos, K. A. Matis, K. S. Triantafyllidis, *ChemSusChem* **2013**, *6*, 110 – 122; c) H. Tadesse, R. Luque, *Energy Environ. Sci.* **2011**, *4*, 3913 – 3929.

[8] a) G. Cheng, P. Varanasi, C. Li, H. Liu, Y. B. Melnichenko, B. A. Simmons, M. S. Kent, S. Singh, *Biomacromolecules* **2011**, *12*, 933 – 941; b) T. Kobayashi, B. Kohn, L. Holmes, R. Faulkner, M. Davis, G. E. Maciel, *Energ. Fuel.* **2011**, *25*, 1790 – 1797.

[9] J. Zhang, Y. Wang, L. Zhang, R. Zhang, G. Liu, G. Cheng, *Bioresour. Technol.* **2014**, *151*, 402 – 405.

[10] Y. Wu, T. Sasaki, S. Irie, K. Sakurai, *Polymer* **2008**, *49*, 2321 – 2327.

[11] a) H. Xie, S. Zhang, S. Li, *Green Chem.* **2006**, *8*, 630 – 633; b) K. Prasad, M.-A. Murakami, Y. Kaneko, A. Takada, Y. Nakamura, J.-i. Kadokawa, *Int. J. Biol. Macromol.* **2009**, *45*, 221 – 225.

[12] F. G. Pearson, R. H. Marchessault, C. Y. Liang, *J. Polym. Sci.* **1960**, *43*, 101 – 116.

[13] a) M. Osada, C. Miura, Y. S. Nakagawa, M. Kaihara, M. Nikaido, K. Totani, *Carbohydr. Polym.* **2012**, *88*, 308 – 312; b) M. Osada, C. Miura, Y. S. Nakagawa, M. Kaihara, M. Nikaido, K. Totani, *Carbohydr. Polym.* **2013**, *92*, 1573 – 1578.

[14] S. F. Tanner, H. Chanzy, M. Vincendon, J. C. Roux, F. Gaill, *Macromolecules* **1990**, *23*, 3576 – 3583.

[15] J. Fernández-Bolaños, B. Felizón, A. Heredia, R. Rodríguez, R. Guillén, A. Jiménez, *Bioresour. Technol.* **2001**, *79*, 53 – 61.

[16] S. M. Hick, C. Griebel, D. T. Restrepo, J. H. Truitt, E. J. Buker, C. Bylda, R. G. Blair, *Green Chem.* **2010**, *12*, 468 – 474.

[17] X. Hu, Y. Du, Y. Tang, Q. Wang, T. Feng, J. Yang, J. F. Kennedy, *Carbohydr. Polym.* **2007**, *70*, 451 – 458.

[18] B. Focher, P. L. Beltrame, A. Naggi, G. Torri, *Carbohydr. Polym.* **1990**, *12*, 405 – 418.

[19] J. T. Scanlon, D. E. Willis, *J. Chromatogr. Sci.* **1985**, *23*, 333 – 340.

[20] S. H. Langer, S. Connell, I. Wender, *J. Org. Chem.* **1958**, *23*, 50 – 58.

Manuscript received: July 20, 2015
Revised: August 21, 2015
Accepted Article published: August 25, 2015
Final Article published: September 7, 2015